Tribo-Mechanical Investigation and Anti-Corrosion Properties of Zn-TiO$_2$ Thin Film Composite Coatings from Electrolytic Chloride Bath.

O. S. I. Fayomi[1,2,*], A. P .I. Popoola[1] and C.A. Loto[1,2]

[1]Department of Chemical, Metallurgical and Materials Engineering, Tshwane University of Technology, P.M.B. X680, Pretoria, SOUTH AFRICA
[2]Department of Mechanical Engineering, Covenant University, Ota, Ogun State, NIGERIA
[*]E-mail: ojosundayfayomi3@gmail.com

Zn-TiO$_2$ (Zn-Ti) composite films were produced on mild steel substrate by electro-deposition from zinc based chloride solutions. The thin film coating was investigated using scanning electron microscopy coupled with energy dispersive spectroscopy (SEM/EDS), x-ray diffraction and atomic force microscopy (AFM). The anti-corrosion behaviour in 3.65% NaCl medium were studied using potentiodynamic polarization technique and characterized by high resolution optical microscope (HR-OPM). The wear and the hardness properties of the composite coatings were measure with high diamond microhardness tester and reciprocating sliding tester respectively. Experimental results show that co-deposited TiO$_2$ particle provides new orientation of metal matrix and modified the surface structure which contributed maximally to the increase in hardness and wear resistance. More so, increase in anti-corrosion property of all the deposits fabricated is attributed to the formation of new phases, surface homogeneity of the developed coating and the thin oxide films of Ti.

Keywords: Zn-Ti, composite coatings, thin films, tribology, corrosion

1. INTRODUCTION

Over the years, electrolytic depositions have been the preferred method due to their bonding characteristics, texture, thickness ratio and low cost over other techniques [1-4]. The widespread depositions then have been through single coating system of Zn, Ni, Co to mention but a few on mild steel substrates. Failure obtained has been a result of non durability in intense corrosive and wear environments and this has limited its effectiveness. To improve this drawback, composite depositions have been seen as alternative for enhancing zinc coatings properties [5-12]. Composite deposition is a unique trend for depositing particles of metallic and non-metallic alloys/compounds in insoluble form

or ceramics and polymers forms into electrolytic bath for specific functions, chemical and mechanical properties [13-18]. Evolution of based materials containing composite and ceramics like ZnO, TiO_2, Al_2O_3, Fe_2O_3, Cr_2O_3 SiO_2 ZrO_2 has proved to give excellent oxidation stability and tribological resistance [14-22]. Though, report on TiO_2 composite particle has been substantial with focus on its corrosion and morphological behaviors and not on their mechanical resistance properties [18]. It is evident that for a material to be beneficial for industrial applications not only its corrosion behavior likewise its mechanical properties or more precisely its surface dependent properties should be studied [22-24]. In view of this, Zn-TiO_2 composite coatings will be fabricated through electrolytic deposition and further characterize the structure, corrosion properties and study the mechanical (Hardness and Wear) behavior.

2. EXPERIMENTAL PROCEDURE

2.1. Preparation of Substrates

Mild steel of (40 mm x 20 mm x 1mm) commercially sourced flat sheet was used as cathode substrate and 99.5% zinc plate of (30 mm x 20 mm x 1mm) were prepared as anodes. The surface preparation was performed with different grade of emery paper as described in our previous studies [3]. The sample were properly cleaned with sodium carbonate, pickled and activated with 10% HCl at ambient temperature for 10 second then followed by instant rinsing in deionized water. Table 1 show the spectrometer chemical analysis of the mild steel subtract used for this study.

Table 1. Chemical composition of mild steel used (wt%)

Element	C	Mn	Si	P	S	Al	Ni	Fe
Composition	0.15	0.45	0.18	0.01	0.031	0.005	0.008	Balance

2.2. Material Composition and Formation:

Table 2. Processed parameter for Zn-TiO_2 chloride bath formulation

Composition	Mass concentration (g/L)
Zn	75
Al	30
KCl	50
Boric Acid	10
TiO_2	7g-13g
ZnCl	75
pH	4.8
Voltage	0.3-0.5V
Time	20 min.
Tempt	40°C

Zn-TiO$_2$ composite coating was produced in a single cell containing two zinc anode and single cathode electrodes as described schematically in fig 1. The distance between the anode and the cathode is 15mm. Before the plating, All chemical used are analytical analar grade and de-ionized water were used in all solution admixed and preheat at 40°C. The processed parameters and bath composition admixed used for the coating is shown in table 2 and 3. The choice of the deposition parameter is in line with the preliminary study and our previous work [23]

The set electrodes were connected to the direct current via a rectifier at varying applied potential and current density between 0.3V-0.5V at 2A for 20 minutes constant time. The plating was done, rinsed in distilled water and samples were air-dried thereafter sectioned for characterization.

Table 3. Itinerary bath composition of Zn-TiO$_2$-Cl alloy co-deposition

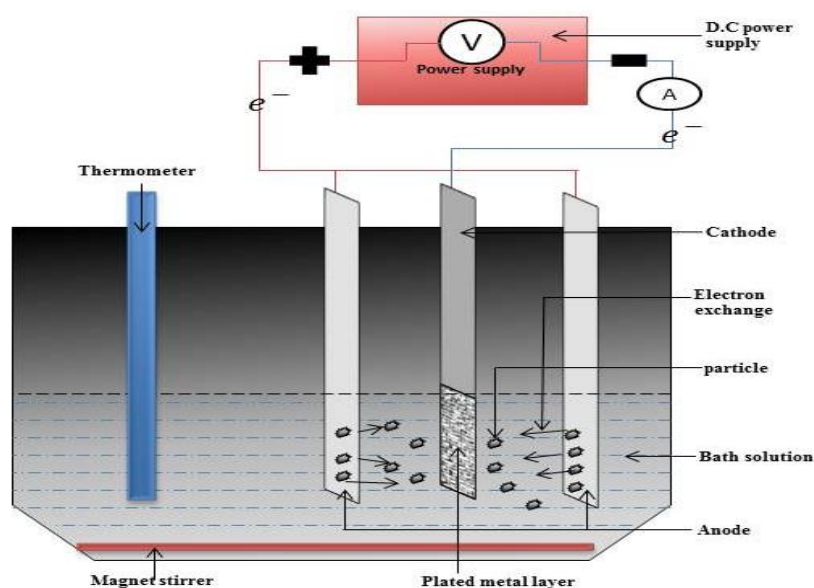| Sample Order	Material sample	Time of deposition (min)	Potential (V)	Current (A)	Con. of additive (g)
Blank	-	-	-	-	-
Sample 1	Zn--7Ti-0.3V-Cl	20	0.3	2A	7
Sample 2	Zn--7Ti-0.5V-Cl	20	0.5	2A	7
Sample 3	Zn--13Ti-0.3V-Cl	20	0.3	2A	13
Sample 4	Zn--13Ti-0.5V-Cl	20	0.5	2A	13

Figure 1. Schematic diagram of electrodeposited system

2.3. Characterization of Coating

The composite coating obtained was characterized with VEGA TESCAN Scanning electron microscope equipped with EDS. The phase change was verified with XRD. Micro-hardness studies were carried out using a Diamond pyramid indenter EMCO Test Dura-scan 10 micro-hardness testers at a load of 10 g for a period of 20 s. The micro-hardness trend was measured across the plated surface in an interval of 20μm

2.4. Friction and wear tests

The tribological properties of the deposited binary alloy fabricated were measured using CERT UMT-2 muiti-functional tribological tester at ambient temperature of $25^{o}C$ with schematic diagram as shown in fig. 2. The reciprocating sliding tests was carried out with a load of 5N, constant speed of 5mm/s, displacement amplitude of 2mm in 20minutes. A Si_3N_4 ball (4mm in diameter, HV 50g-1600) was chosen as counter body for the evaluation of tribological behavior of the coated sample. The dimension of the wear specimen is 2cm by 1.5cm as prescribed by the specimen holder. After the wear test, the structure of the wear scar and film worn tracks are further examined with the help of high optic Nikon Optical microscope (OPM) and scanning electron microscope couple with energy dispersive spectroscopy (VEGAS-TESCAN SEM/EDS).
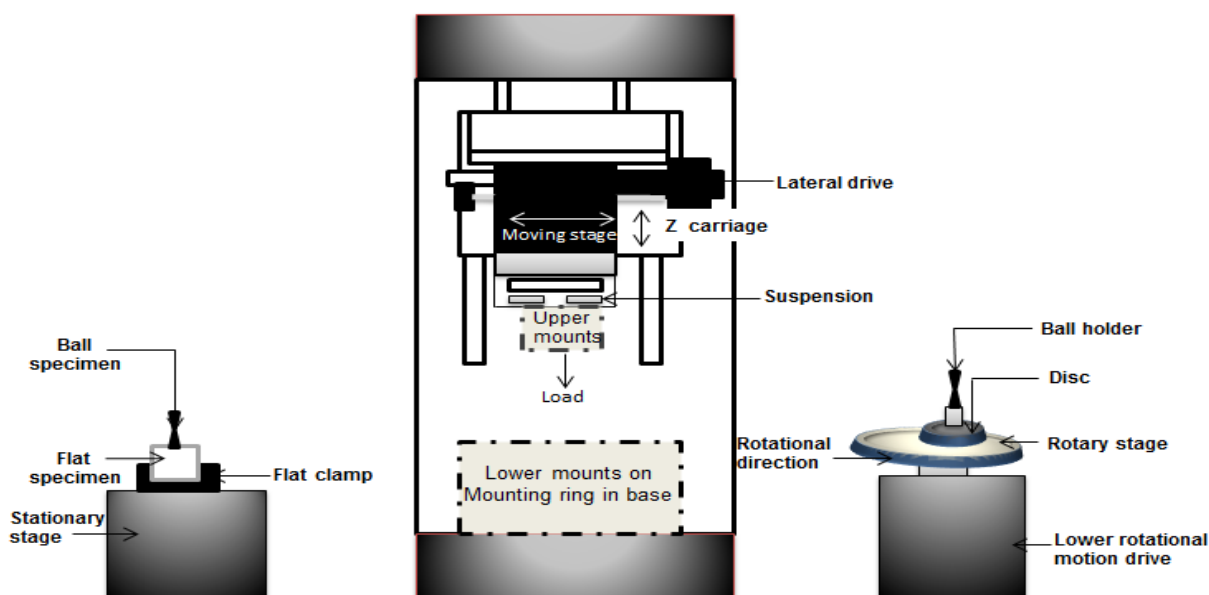

Figure 2. Schematic view of reciprocating sliding friction CERT UMT-2 test system

2.5. Electrochemical test

Autolab PGSTAT 101 Metrohm potentiostat with a three-electrode cell assembly in a 3.65% NaCl static solution at $40^{o}C$ was used to examine the anti-corrosion behavior of the composite

coatings. The developed composite was the working electrode, platinum electrode was used as counter electrode and Ag/AgCl was used as reference electrode. The anodic and cathodic polarization curves were recorded by a constant scan rate of 0.012 V/s which was fixed from ±1.5 mV.

3. RESULTS AND DISCUSSION

3.1. Influence of Composition on Coating Thickness:

The effect of the deposit condition expecially the additive concentration and applied potential could be seen on the resulting zinc-titanium coating thickness and weight gain under a fixed time. Interestingly, there is a significant correlation between the composite concentration and the deposition potential. As the voltage increases, the coating thickness change automatically with a difference of 79 μm and 120 μm at both 7g and 13g mass of additive respectively. Infact, one can obviously fell the impact of additive on the deposit. At 0.5V with 7g induced composite particulate, 186μm thickness was obtained. When the particle was increased to 13g, a rise in the coating thickness values of 263μm was attained; with a justifiable increase of 77μm. The same trend also applies to the degree of weight gain obtained. Although, such is expected, the reason being that transport of particle as a result of adsorption and total diffusion during particle inclusion into metallic deposit can lead to improved texture and weight gain [18]. More so, since composite characteristics are influenced by the current induced, bath formation, applied voltage, pH and particle concentration (see table 4.14), it is expected that such should influence the amount of deposit entrapped which could give desire coating thickness and weight gain needed [14].

3.2. Characterization of Zn-TiO₂ Coatings: Atomic force microscope (Zn-TiO₂ chloride deposition)

Atomic force microscopy examination was carried out on Zn-TiO$_2$ films obtained at varied concentrations of composite (7g/L and 13g/L) on the zinc based alloy as illustrated in Figures 3 and 4 respectively. The micrographs revealed to some extent an improved topography of zinc-titanium matrix. Comparative studies between Zn-7Ti-0.3V-Cl and Zn-13Ti-0.3V-Cl thin films deposits from Zn-Ti matrix as described in table 3 show that Zn-7Ti-0.3V-Cl possesses non-homogeneous surfaces with defects within interface. For Zn-13Ti-0.3V-Cl thin film the topography was quite uniform with coalesce characteristics (Figure 4). Although [1] reported that the presence of TiO$_2$ could result to more nucleation site which further retard and control the crystal growth. Therefore an enhancement in the structural properties of Zn-13Ti-0.3V-Cl is traced to the physical barriers produced by TiO$_2$ in relation to the throwing potential applied for the deposit. It is important to mention that diffusion and adsorption are critical phenomena in co-deposition of metallic particle and composite [20]. Though, the influence of temperature variation was not considered in this study, but thermodynamic movement of Ti molecule at 40°C could be found to help in the stability and dispersion of the deposits of Zn-13Ti-0.3V-Cl with adsorbed atom wanders at the rich zinc lattices to fill up the gaps and micron holes.
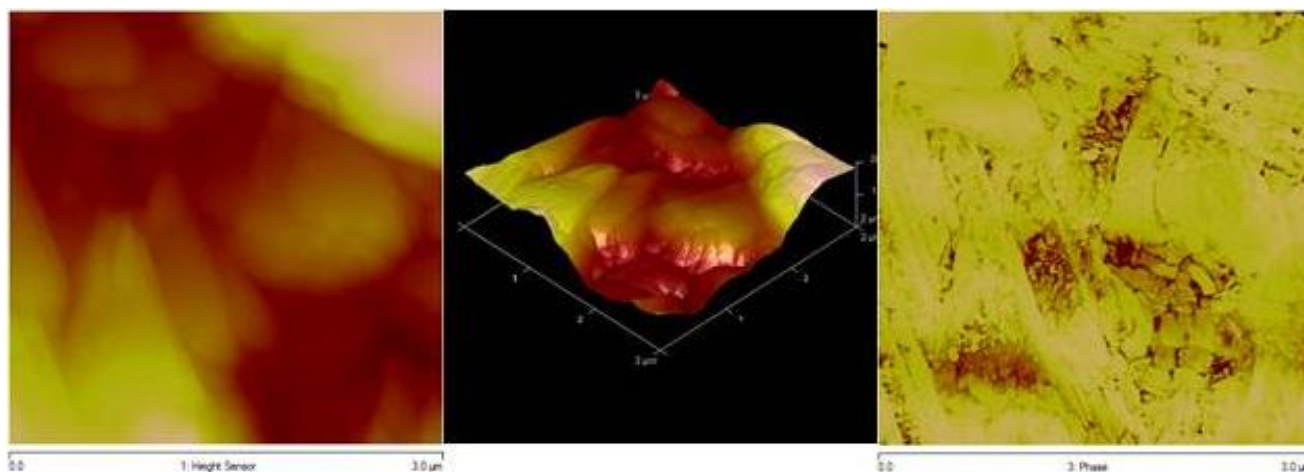
Figure 3. AFM images of the Zn-7Ti- film obtained for (a) 2-D image, (b) 3-D relief image and (c) roughness analysis.
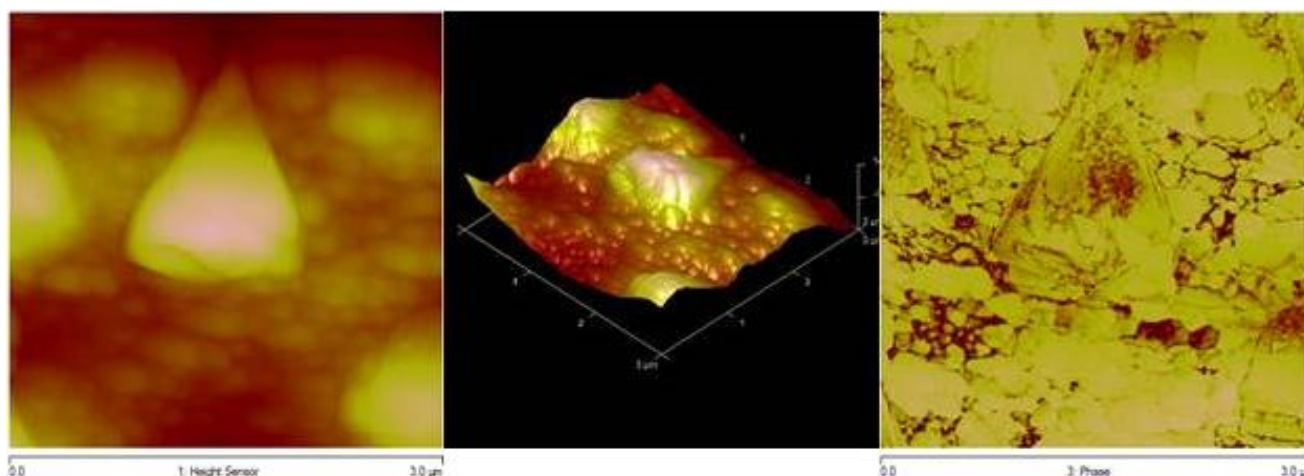

Figure 4. AFM images of the Zn-13Ti film obtained for (a) 2-D image, (b) 3-D relief image and (c) roughness analysis.

3.3. Solid XRD analysis for Zn-TiO$_2$ deposited mild steel

Phase identification of composite coating was performed by means of x-ray diffraction analysis for Zn-TiO$_2$ with consideration on Zn-7Ti-0.3V-Cl and Zn-13Ti-0.3V-Cl thin film deposit. The matrix patterns are presented in Figures 5 and 6 respectively. The analysis of the deposits points to the metal matrix modification of Zn, ZnO to TiO$_2$ and the formation of different intermetallic phases. The coating electrodeposited with Zn-7Ti-0.3V-Cl was found to possess intermetallic phase of Zn, Ti, and Zn$_2$Ti$_3$. The titanium content in the major phase was very small thus the peak are weak and found in a single form below the braggs angle.
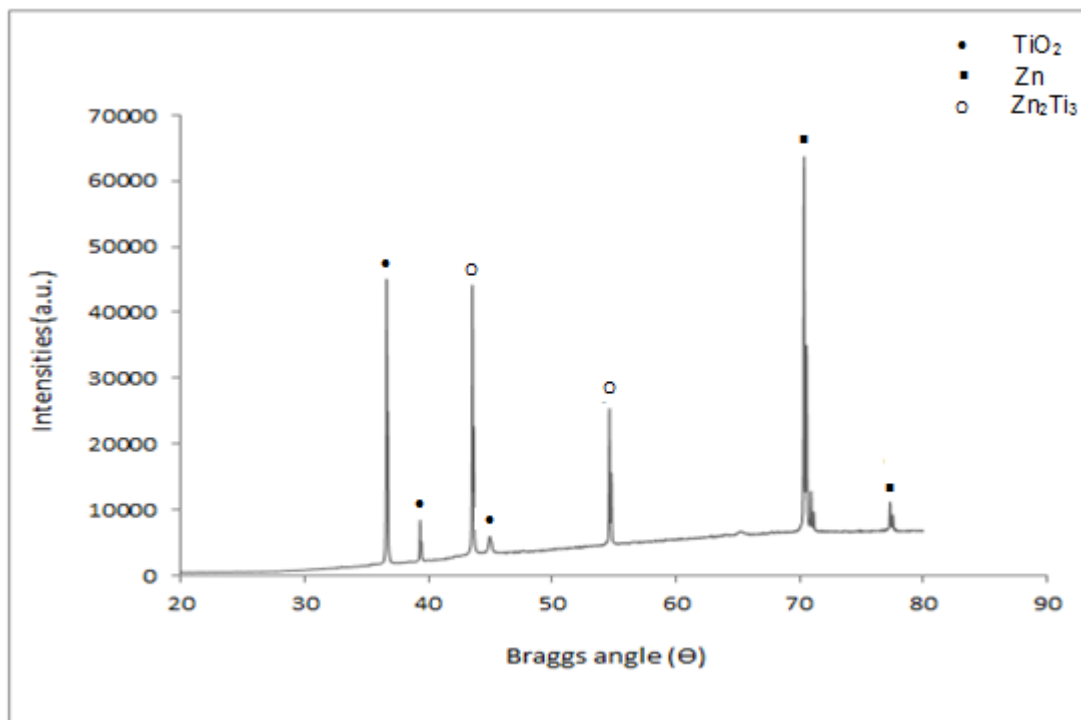
Figure 5. Solid X-ray diffraction profile for Zn-7Ti-Cl-0.3V thin film.

Although no carbon peak was found. On the other hand, significant height of titanium peak was seen with Zn-13Ti-0.3V-Cl coating with Zn, TiO_2, and ZnTi, phases. The Ti content on the later tends toward noble region thereby given rise to ZnO.
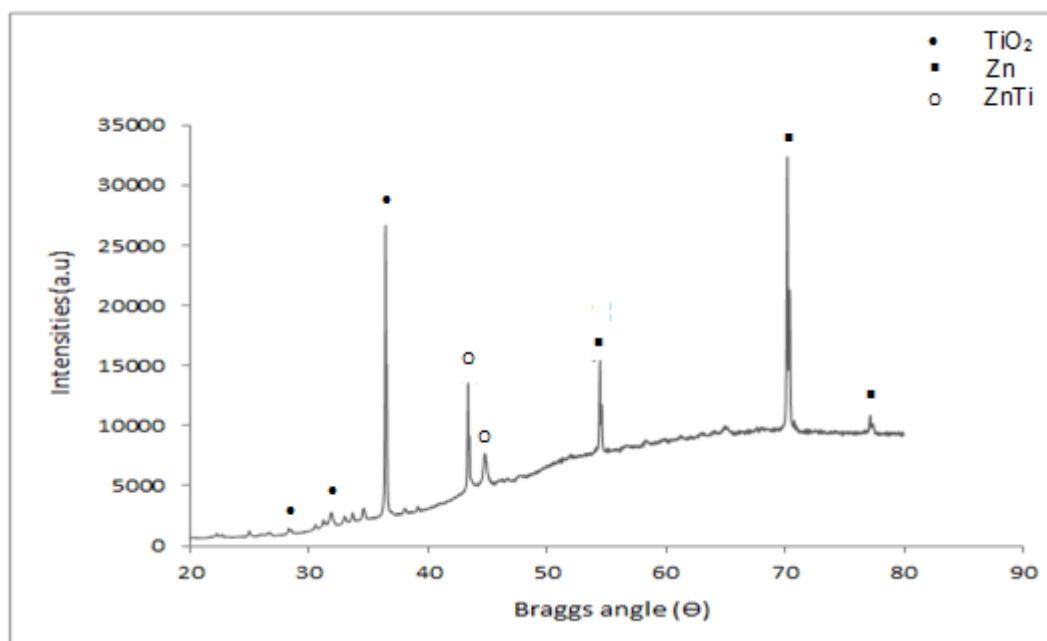

Figure 6. Solid X-ray diffraction profile for Zn-13Ti-Cl-0.5V thin film.

Interestingly [13] attested that TiO_2 composite incorporated into the Zn matrix can act as a seed for the growth of ZnO which could result into better modification and excellent properties. Another silent observation of appreciable phase of Zn-13Ti-0.3V-Cl as seen in figure 6 is the peak width of the matrix with broader intensity which is sometimes attributed to reduction in grain size of the deposit [1].

To complement the phase patterns, figure 7 show the ramma pattern of $Zn-TiO_2$ especially with Zn-13Ti-0.3V-Cl matrix. With the incorporation of the composite Ti particle, the Zn content on the lattice reduces; thereby shift the ramma intensity progressively.
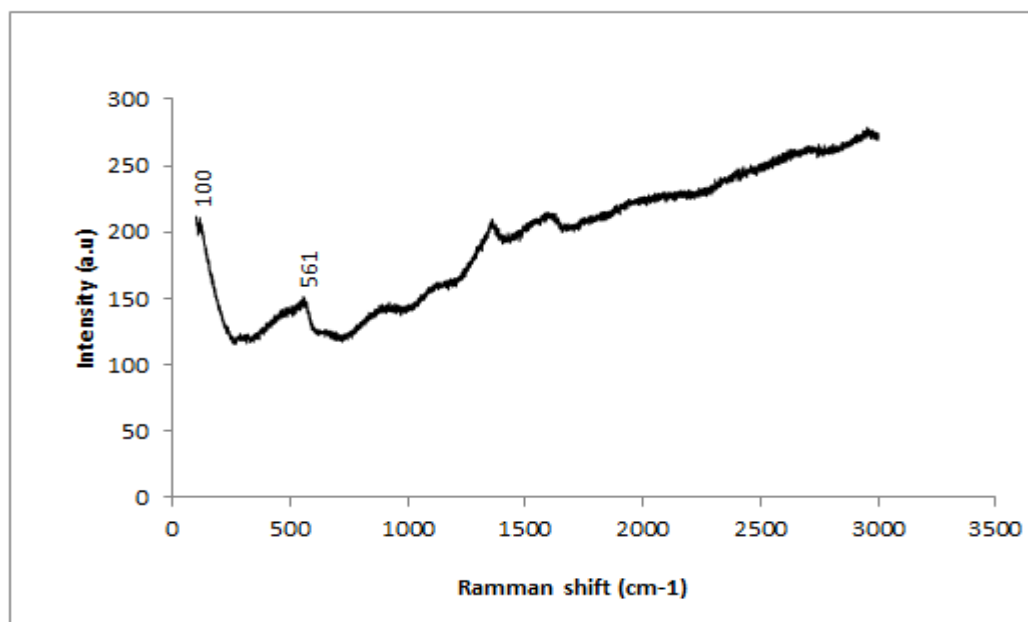

Figure 7. Ramma profile for Zn-7Ti-Cl-0.3V thin film.

3.4. SEM/EDS analysis of $Zn-TiO_2$ deposited mild steel

Figure 8-9 shows the surface morphology of the fabricated zinc-titanium layers prepared in 20 minutes of DC deposition with different potential values. Comparing the structure obtained from Zn-7Ti-0.3V-Cl thin film and Zn-13Ti-0.5V-Cl deposit, coating compose of crystals were seen with the growth dominated by Zn. it can be observed that the Zn films completely covered the substrate. The structural evolution of the coating was not perfect as expected with Zn-7Ti-0.3V-Cl (see figure 8) although the deposit had coarse crystal size. The condition for buildup of crystal entails a high surface-diffusion rate, deposition parameter and concentration of induced additive. With Zn^{2+} dominating over the embedded Ti particulate, zinc crystallite in hexagonal shape was seen. In addition, the figure revealed that at Zn-7Ti-0.3V-Cl the effect of TiO_2 on the matrix has little modification on the coating. The EDS confirm traces of Ti addition in the deposits.
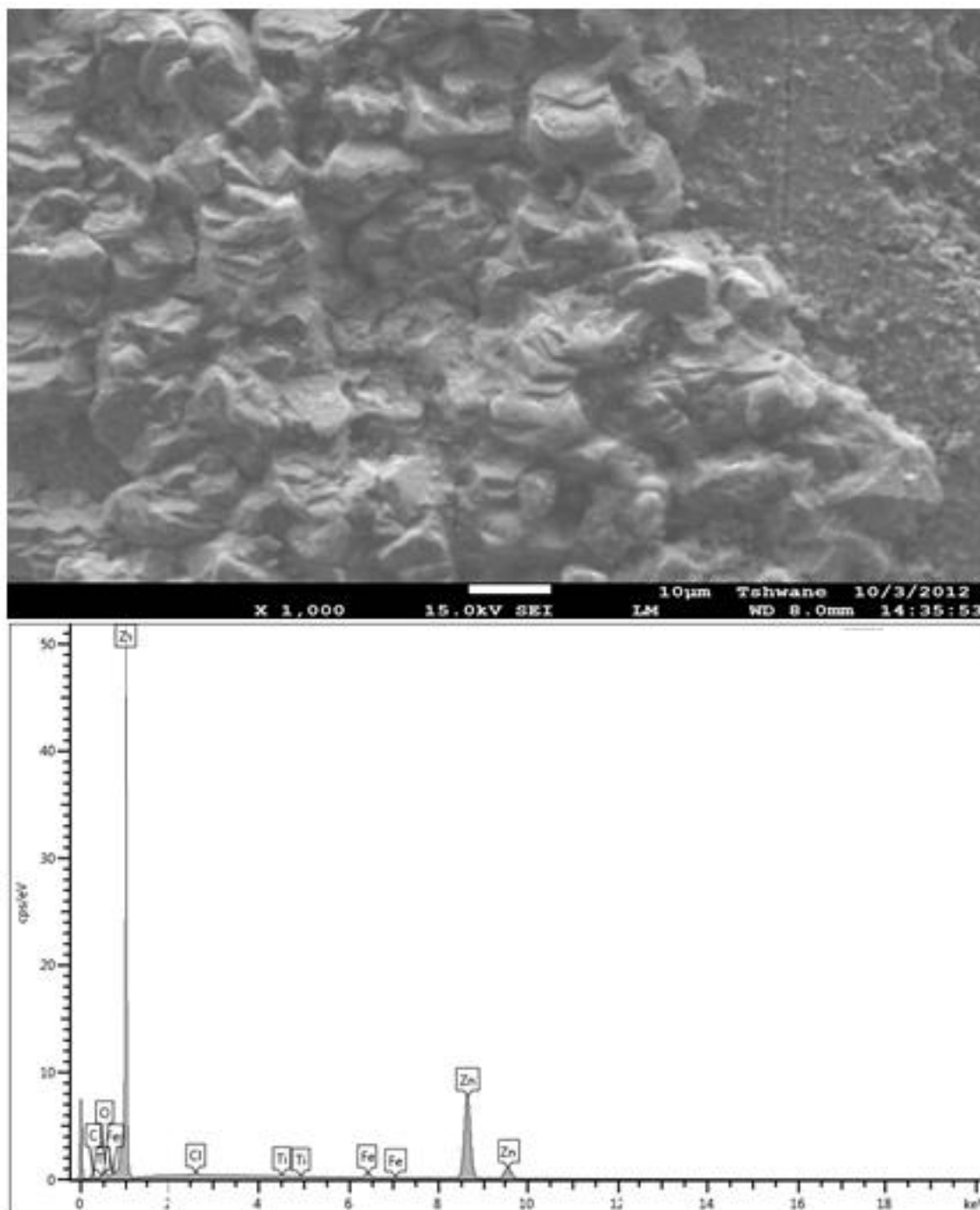
Figure 8. SEM/EDS showing the surface morphology of Zn-7Ti-0.3Vchloride deposited sample

Figure 9 contains SEM images of the Zn-13Ti-0.5V-Cl composite matrix coating prepared at 13g/L TiO_2 concentration in zinc bath. This structure gave a unique morphology that is distinct from the deposit at 7glL (figure 8). It can be seen that the incorporation of the composite particle in the zinc thin film coating favors structure modification. This result is also in agreement with the report by [24] validating the effect of the presence on zinc structure.
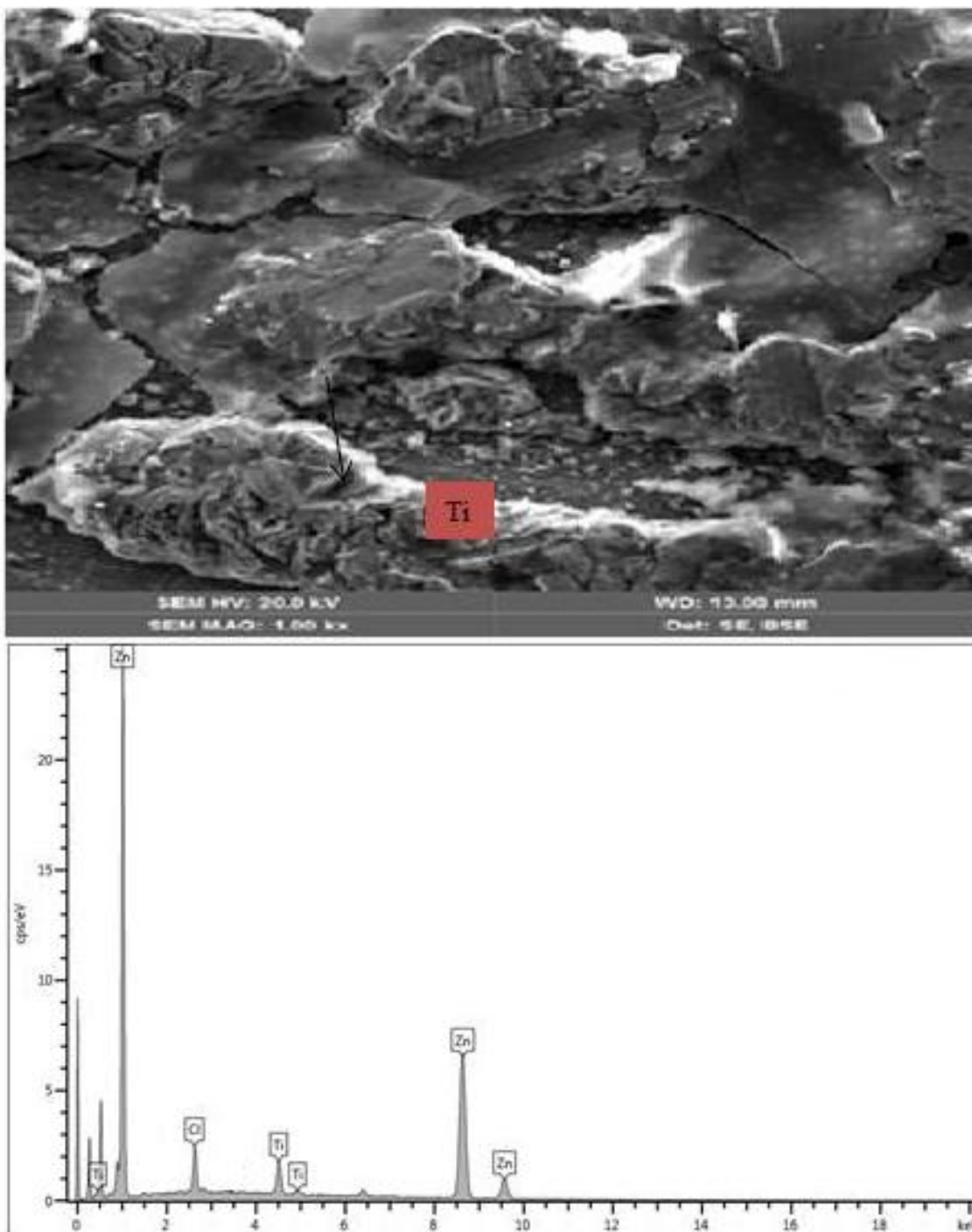
Figure 9. SEM/EDS showing the surface morphology of Zn-13Ti-0.5Vchloride deposited sample

Furthermore, from the EDS studies widespread of Ti particulate were seen. In view of this we assumed that addition of Ti lead to the formation of Ti-rich layer at the zinc steel interface as described by [12]. However it is essential to mention that particle content is not the only factor that drastically influences the morphological properties but obviously mechanism of coating relies on reinforced or particle strengthening characteristics [10]. To confirm the potentials of the deposits at lower

magnification, figures 10a-b shows the optical micrographs of the binary system of Zn-7Ti-Cl-0.3V matrix and composite coating produced at Zn-13Ti-Cl-0.5V respectively.
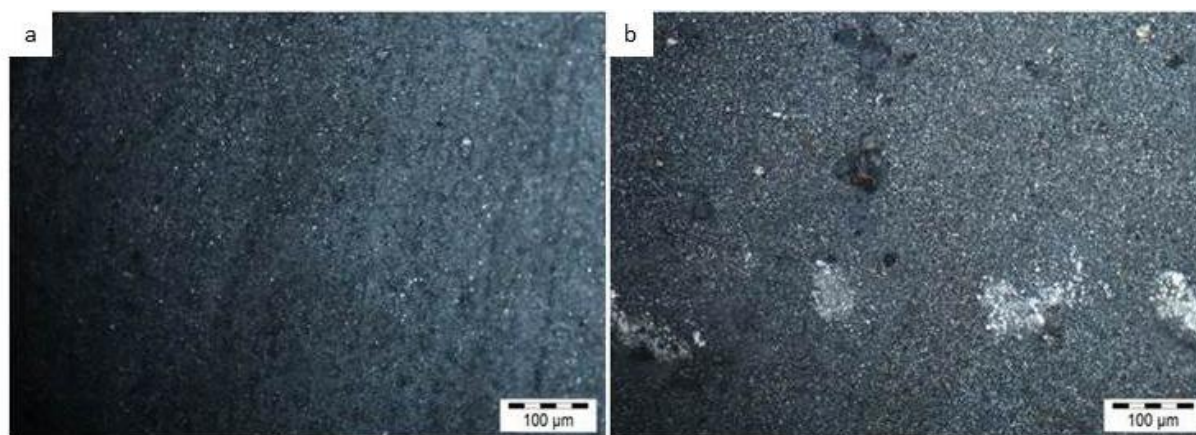

Figure 10. Optical micrograph of the morphology for a) Zn-7Ti-0.3V b) Zn-13Ti-0.5V chloride deposited mild steel.

In all, the nature of the deposit is found adherent, homogeneous defect free surfaces especially with composite coating produced at Zn-13Ti-Cl-0.5V.

3.5. Microhardness Analysis of Zn-TiO$_2$ Deposited Mild Steel

The qualitative average microhardness result for the Zn-TiO$_2$ composite coating at various bath composition and parameter are shown in figure 11. In general, as-deposited composite coatings in all matrixes had higher microhardness than as-received sample. It can be suggested that TiO$_2$ in the composite coating could act as a strong barrier to disallow deformation of the solid matrix and further enhance the hardness property. Obviously we see that deposition rate reduces with increase in microhardness and TiO$_2$ concentrations. More surprisingly is that at beyond 7glL there is no noticeable increase as changes which were expected but rather a slight reduction in the hardness value. The lower potential had obtained a better hardness in all composite coating matrixes than coating fabricated at 0.5V.

Although, [8] reported, that the deposition rate and the microhardness increase with increase with nano-composite concentration and further stated that the microhardness change is not obvious if the nano-particle concentration is over 10glL. In view of this, we assumed that the characteristics of individual composite and the current density to potential applied for a particular coating could result into the type of hardness value obtained. This supposition is confirmed by [24] report that the adsorption of particle at the active site will inhibit the growth of the metal crystals by producing fine grained structure but high amount of particle incorporation are not directly correlated to zinc crystallite size. At this point, changes in microhardness are supported with the co-deposition parameter and not the concentration of composite induced in all cases. The hardness profile data for all the samples

shows significant average increase. Zn-7Ti-Cl-0.3V 5 has the highest value of hardness with 153 HVN; (see figure 11).
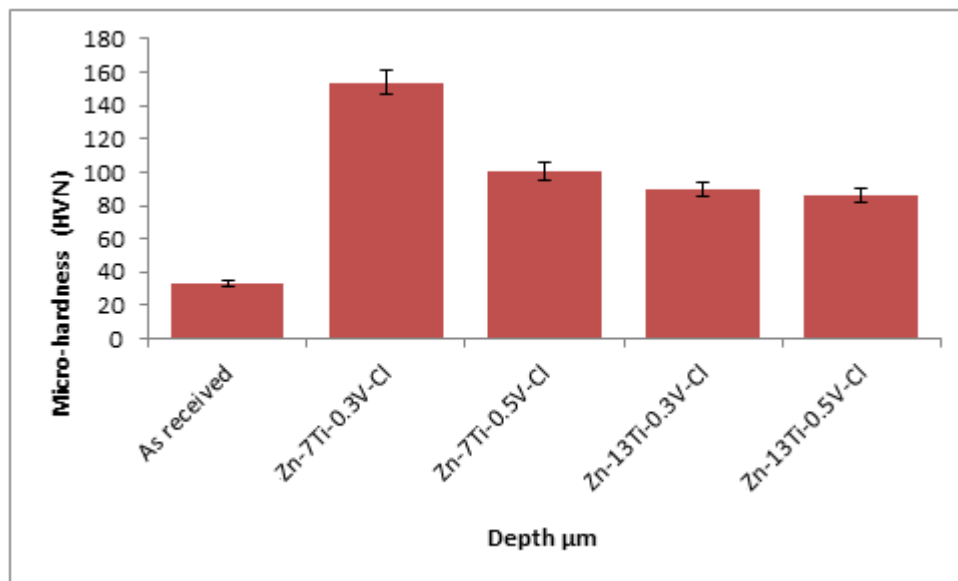

Figure 11. The microhardness/depth profile for Zn-Ti chloride deposited sample

The microhardness value for the substrate material is 33.5 HVN. For Zn-7Ti-Cl-0.3V sample is 100 HVN, for Zn-13Ti-Cl-0.3V sample is 84.4 HVN, and Zn-13Ti-Cl-0.5V is 85.7 HVN. In general, this improvement in hardness (double the microhardness of substrate) was attributed to the formation of adhesive properties on the substrate and the phases formed coupled with microstructural grain refinement.

3.6. Wear Rate Evaluation of Zn-TiO₂ Deposited Mild Steel

Figure 12 show comparative tribological behavior of total wear loss of all matrix composite and as-received mild steel subtrate. From all evidence results show that wear resistance attained by electrodeposition composite alloy was remarkable. The rate of wear loss is very high for the as-received sample. It is evident that the incorporation of induced TiO_2 particle in Zn matrix improves the plastic deformation resistance and reduces wear volume loss. However, taking in consideration the percentage of additive induce, Zn-7Ti-Cl-0.3V matrix at 7g/L produce an excellent wear resistance among composite alloy. Although alloy fabricated at Zn-13Ti-Cl-0.5V was expected to provide a more significant properties considering its higher percentage of induce composite and applied potential. To support the performance of Zn-7Ti-Cl-0.3V [15] affirmed in its report that doping certain (moderate) amount of particles increase wear life and in other view addition of excessive particle on Zn matrix film seriously deteriorate tribological resistance due to phase separation. Therefore the possibility of producing a processed coating with good wear properties is not a function of excessively inoculated particle but exact modifier that could improve adhesion and mechanical stability of the thin film on the

substrate which will further guarantee wear resistance. In general, all composite thin film coating performance shows satisfactory behavior over the as-received.
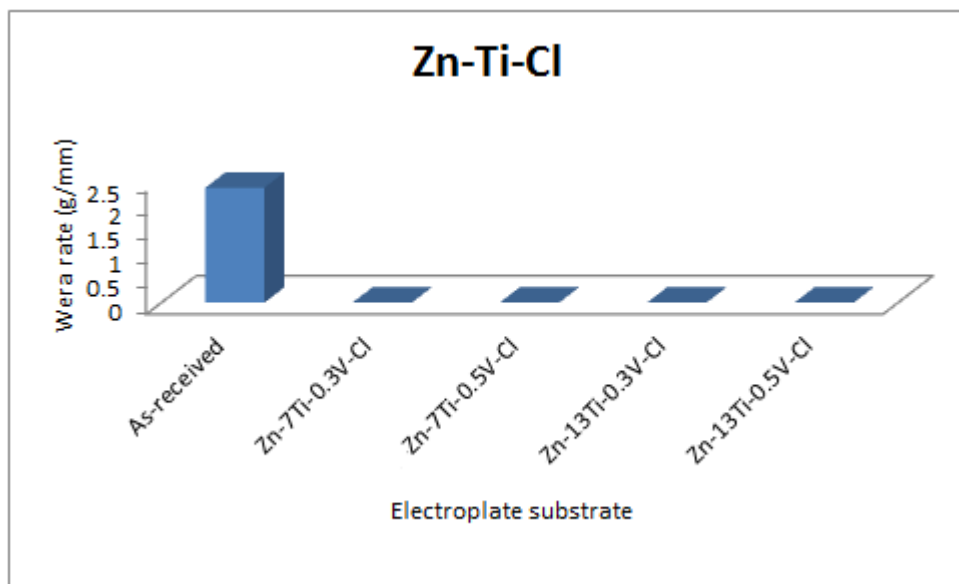

Figure 12. Variation of the wear rate with time of Zn-Ti-Cl

To qualitatively observe the friction and the tribological behavior further, figure 13 and 14 shows the friction coefficient of the best matrix (Zn-7Ti-Cl-0.3V) from the Zn-TiO$_2$ alloy against the as-received sample under non lubricated condition at room temperature. It can be seen that Zn-TiO$_2$ exhibited a lower friction coefficient against the substrate as the time and the sliding velocity progress (see figure 13 and 14).
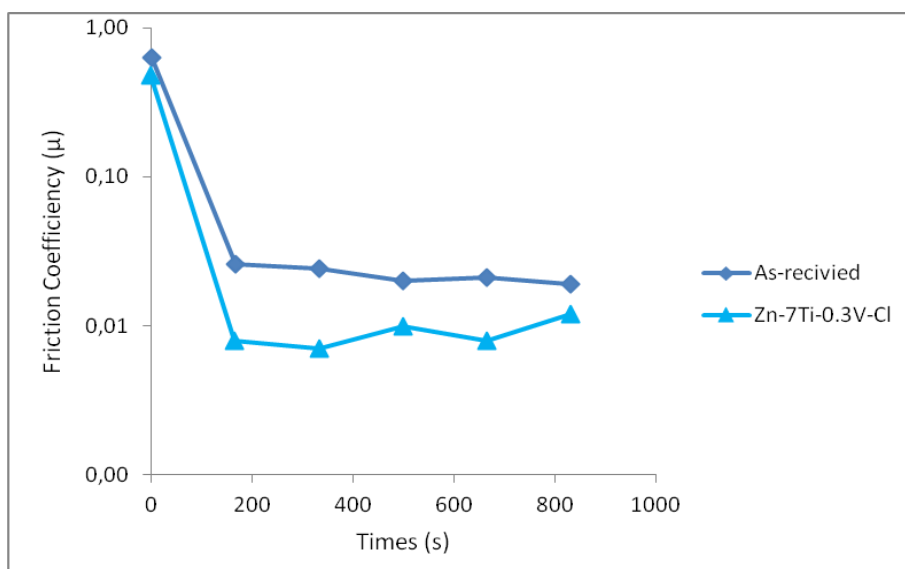

Figure 13. Variation of wear friction co-efficient against time for Zn-7Ti-0.3V Chloride deposited sample
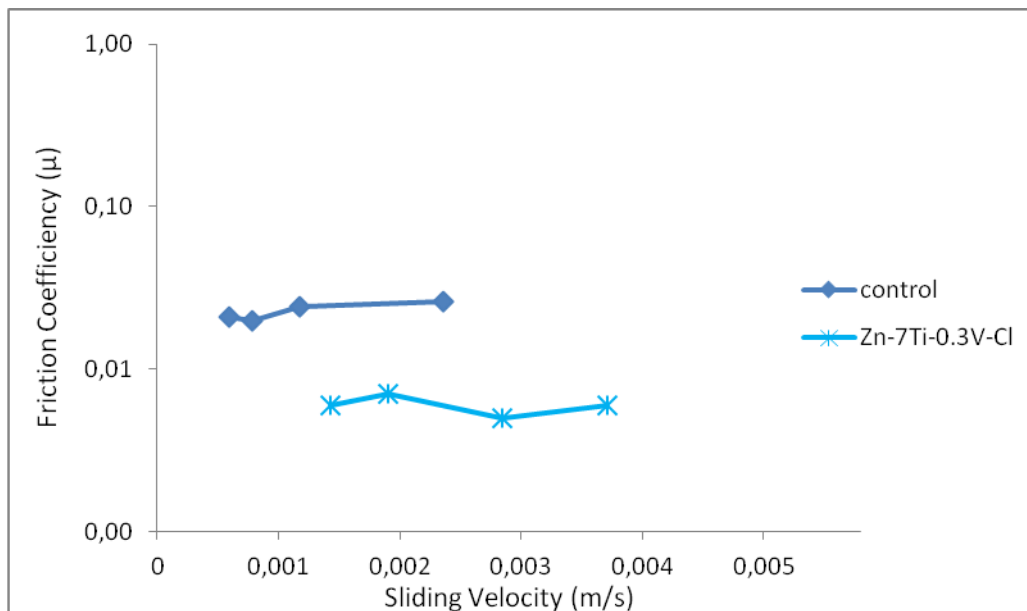
Figure 14. Variation of wear friction co-efficient against sliding velocity for Zn-7Ti-0.3V Chloride deposited sample

It is more important to mention at this point that possible crystal size oriented within the interface of the Zn matrix have led to the composite thin film coating having reduce friction coefficient. Also [10] affirmed that the resulting effects for this lower behavior are attributed to change in microstructure of the thin films.

The failure and worn surfaces of the obtained fabricated coating are observed from SEM and OM images. The wear morphology of the as-received material failed with crack, groove and micro-debris as shown in figure 15.
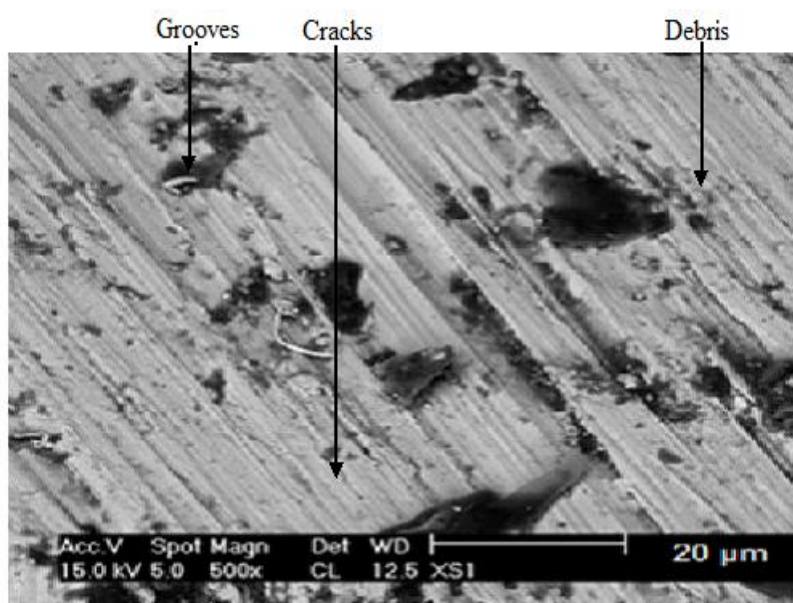

Figure 15. SEM spectrum of the wear scar on the as-received sample

From the selected composite coating matrix, the composite coating show a good resistance to plastic deformation with few groove especially for Zn-7Ti-Cl-0.3V as indicated in figure 16. Although, [17] mentioned that a coating with poor adhesion simultaneously show failure. That is, the degree of failure can be justified by the adhesion properties during coating. In view of this few debris indicated with coating produced by Zn-13Ti-Cl-0.5V in figure 16b might be traced to this adhesion phenomena
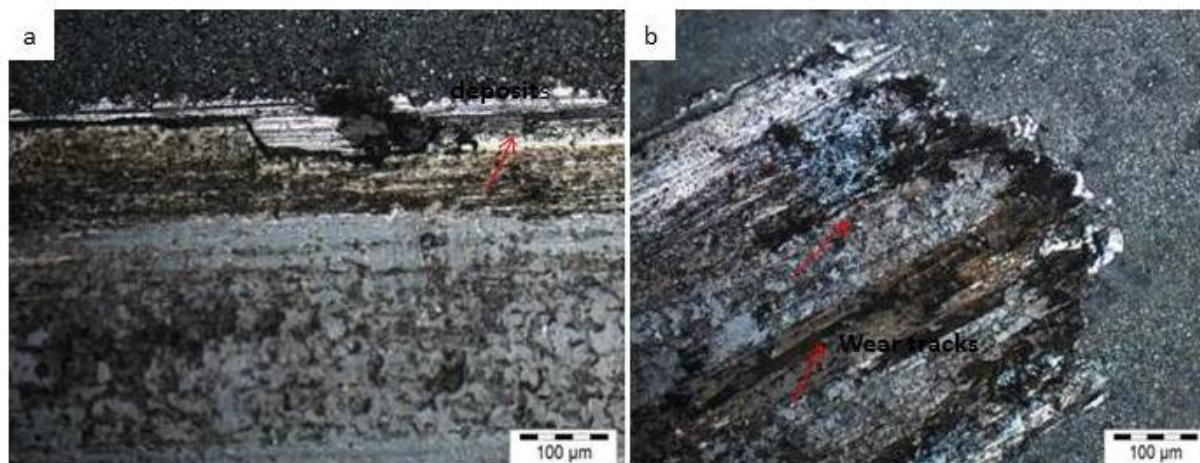

Figure 16. Micrograph of the wear scar for a] Zn-7Ti and b] Zn-13Ti chloride deposited sample

3.7. Electrochemical Test Result of Zn-TiO$_2$ Chloride Deposited Mild Steel

Polarization examination was performed on Zn-TiO$_2$ alloy matrix to verify the protective ability and the reactivity of the deposited composite alloy in 3.65% NaCl environment. From the Tafel plots the corrosion potential (E_{corr}) and corrosion current density (I_{corr}) were examined. The cathodic and anodic polarization curves for the composite coating matrix were shown in Figure 17. From observation, a sudden rise in current density occurs with as-received sample but for all composite coated samples the current density was gradual. For comparison purposes among the composite deposited matrix, the result of Zn-7Ti-Cl-0.3V alloy was found to have produced improved polarization potential with (-1.15814 V).

The potential was observed to shift towards less negative region. Next to the best produced alloy is Zn-13Ti-Cl-0.3V composite alloy with a slight potential lower than the formal (-1.17035 V) as it moves toward the positive sight. This very excellent behavior existing among all composite alloys against as-received sample suggest that TiO$_2$ particles incorporated in the fabricated Zn-Ti matrix made the penetration of Cl$^-$ dissolution difficult. Another important consideration is the degree of anti-corrosion property in relation to the percentage of additive. Hence, slight dissolution observed from composite alloy is the results of dissolution tendency of Zn dominate among the alloy.

The result of polarization measurements for the specimens investigated are summarized in Table 4. The as-received sample had a corrosion current of 2.04x10^{-3} A and a corrosion rate of about 4.1 mm/yr. which is expected due to lack of surface protection. This occurrence was ascribed to the high anodic potential reached by the sample, absorption of the halide ion on the oxide film which took

place at the oxide solution interface and the formation of basic oxide. For Zn-7Ti-Cl-0.3V, i_{corr} of 2.11×10^{-5} A was attained.

Table 4. Summary of the potentiodynamic polarization results

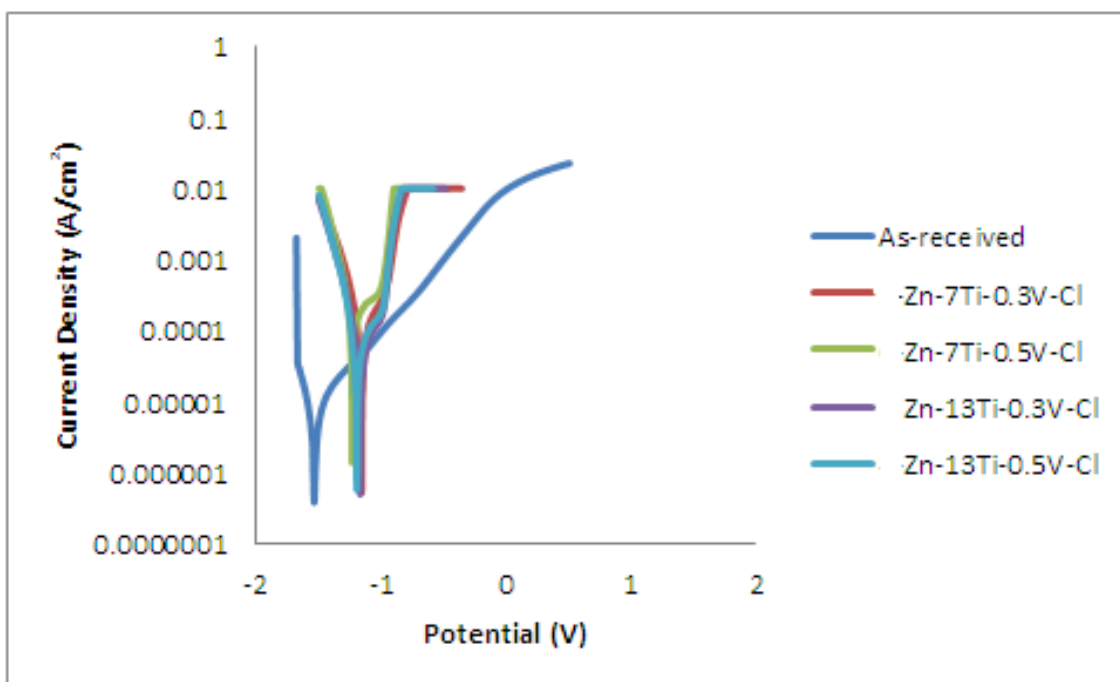| Sample	E_{corr} (V)	i_{corr} (A/cm^2)	$R_p(\Omega)$	Corrosion rate (mm/yr)
As-received	-1.539	7.04E-02	27.60	4.10
Zn-7Ti-0.3V-CI	-1.158	2.11E-05	413.63	0.246
Zn-7Ti-0.5V-CI	-1.234	3.03E-05	222.96	0.352
Zn-13Ti-0.3V-CI	-1.170	5.63E-05	208.56	0.654
Zn-13Ti-0.5-CI	-1.197	589E-0.5	153.32	0.684

Figure 17. Potentiodynamic polarization curves for Zn-Ti chloride deposited mild steel

A two order magnitude decrease in corrosion current against the working sample. However if increase in polarization resistance lead to decrease in current density and corrosion rate as affirmed by [20-21]: the polarization resistance (R_p) result, for For Zn-7Ti-Cl-0.3V which had 4.12×10^2 (Ω), obviously has the highest attained resistance to polarization for all the coated samples. The order of corrosion resistance of the composite sample are Zn-7Ti-Cl-0.3V > Zn-13Ti-Cl-0.3V > Zn-13Ti-Cl-0.5V and Zn-7Ti-Cl-0.5V.
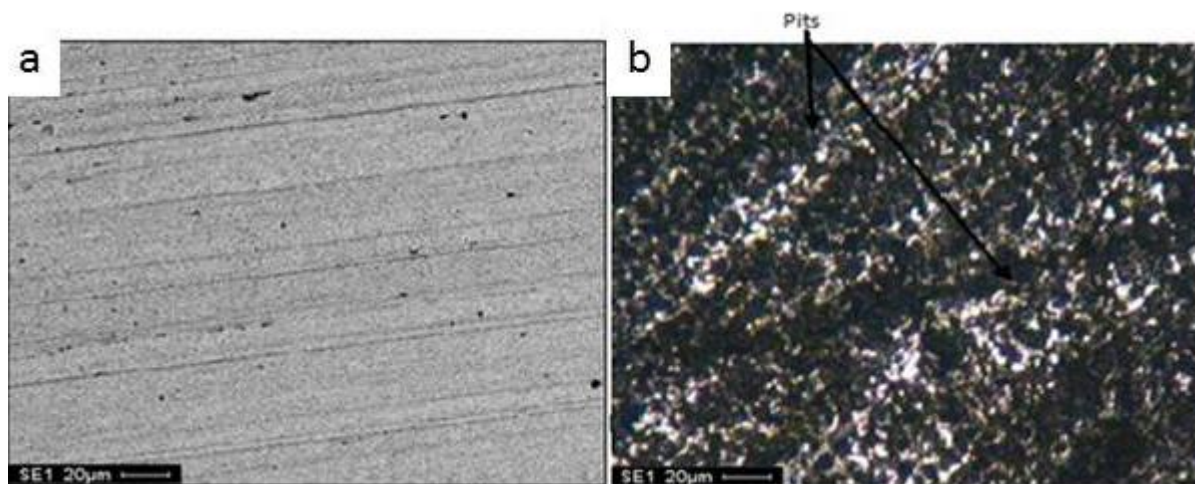
Figure 18. Micrograph of a] as-received sample before corrosion b] after corrosion

To access the stability and surface degradation resulting from Zn-TiO$_2$ selected matrix deposited sample after corrosion, figures 18a-b show the micrograph of the surface and after electrochemical induction. Pit revolved round the surface of the un-protected steel as shown in figure 18b. From all indications, Zn-7Ti-Cl-0.3V –possess non visible corrosion attack as seen from Figure 18c. For Zn-13Ti-Cl-0.3V coatings corrosive product and little pit are within the interfaces. Although, Cl$^-$ impunity on coated matrix above 7glL could result into coating severe degradation as a result of gap and in stability of the coating due to excessive particle induced.
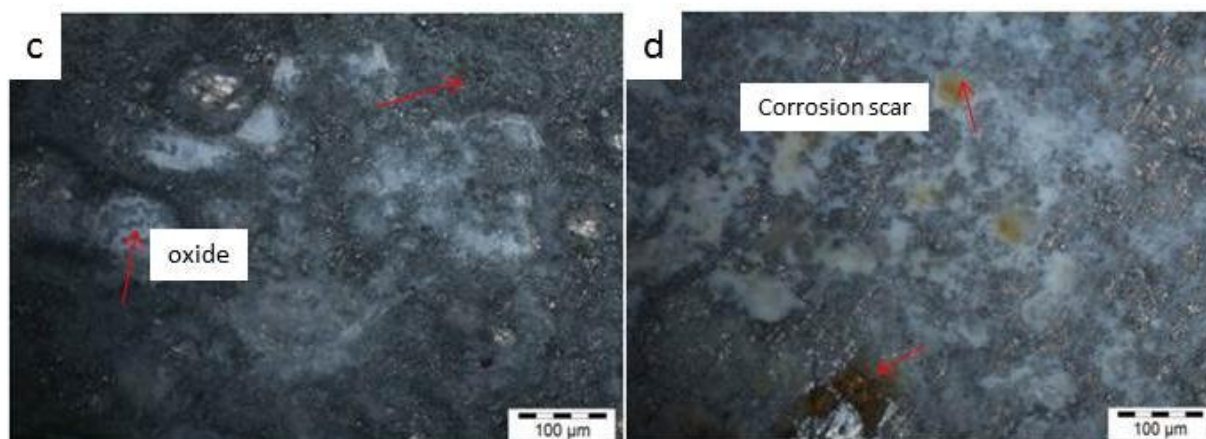

Figure 18. Micrograph of a] Zn-7Ti-Cl-0.3V b] Zn-13Ti-Cl-0.5V chloride deposited mild steel after corrosion.

4. CONCLUSION

✓   Feasible fabrication of binary coating alloy containing Zn-TiO$_2$ matrix was achieved on mild steel. It was seen that by modifying the composition of the electrolyte with additive, the produced

structure displayed strong strengthening behavior with reduced grains as a result of dispersion particulate.

Change in the composition parameters and additive changes the resulting individual morphology, microhardness, tribological resistance, and the friction coefficient of the composite material. The average increase in microhardness for the best improved alloy among the composite deposited series Zn-7Ti-Cl-0.3V 5 has 153 HVN compared to the substrate material with 33.5 HVN. For Zn-7Ti-Cl-0.3V sample microhardness is 100 HVN, for Zn-13Ti-Cl-0.3V sample is 84.4 HVN, and Zn-13Ti-Cl-0.5V is 85.7 HVN. In general, this improvement in hardness (double the microhardness of substrate) was attributed to the formation of adhesive properties on the substrate, the phases formed coupled with microstructural grain refinement.

✓ The finding from the corrosion properties revealed that the composite coatings have good anti-corrosion resistance properties in corrosive media of 3.65% NaCl over mild steel.

✓ The slight pitting corrosion hurt by Zn-13Ti-Cl-0.5V is attributed to fewer ionic migrations of chloride into the surface lattice. In general, all the composite coatings potentials are nobler and the current densities are lower compared to the one obtained from the working mild steel substrate.

References

1. B.M. Praveen, T.V. Venkatesha, *Appl. Surf. Sci.,* 254 (2008) 2418
2. L Chuen-Chang, H. Chi-Ming, *J. Coat. Technol. Rese.* 3 (2006) 99
3. O.S.I Fayomi, A. P. I. Popool, *Int. J. Electrochem. Sci.,* 8 (2013) 11502
4. C. Mohankumar, K. Praveen, V. Venkatesha, K. Vathsala, O. Nayana. *J. Coat. Techno Rese.*, 9 (2012) 71
5. M.M. Abou-Krisha, F.H. Assaf, S.A. El-Naby, *J. Rese .Coat. Technol.,* 6 (2009) 391
6. M.J. Rahman, S.R. Sen, M. Moniruzzaman, K.M. Shorowordi. *J. Mech. Eng., 40 (*2009) 9
7. M. Arici, H. Nazir, A. Aksu, *J. Alloys. Comp., 509* (2011) 1534
8. R. Xu, J. Wang, Z. GUO, H. Wang, *J. Rare. Earth.*, 26 (2008) 579
9. G. Yang, S. Chai, X. Xiong, S. Zhang, L. Yu, P. Zhang., *Trans. Non. Ferro. Metals. Socie. China.* 22 (2012) 366
10. T.G. Wang, D. Jeong, Y. Liu, S. Lyengar, S. Melin, K.H. Kim, *J. Surf. Coat. Technol.,206* (2012) 2638
11. O. Hammami, L. Dhouibi, P. Bercot, E.M. Rezrazi, E. Triki, *Int. J. Corro. Sci.,8* (2012) 1
12. S.M.A. Shibli, F. Chacko, C. Divya, *J. Corros. Sci.*, 52 (2010) 518
13. A. Gomes, T. Frade, I.D. Nogueira, *Curr. Micros. Contri. Advan. Sci. Technol., 2* (2012) 1146
14. O.S.I. Fayomi, M. Abdulwahab, A.P.I. Popoola, *J. Ovonic. Rese., 9* (2013) 123
15. Y. Zhang, B. Huang, P. Li, X, Wang, Y, and Zhang *J. Euro. Ceramic. Socie.*, 58 (2013) 7
16. A. Abdel, M.A. Barakat , R.M. Mohamed, *Appl. Surf.,* 254 (2008) 4577
17. Y,L Su, and W.H Kao, *Trib. Int.* 36 (2003) 11
18. J. Fustes, A.D.A. Gomes, M.I. Silva Pereira, *J. Solid. State. Electrochem.*, 121 (2008) 1435

19. D. Dong, X.H. Chen, W.T. Xiao, G.B. Yang, P.Y. Zhang, *Appl. Surf. Sci., 255* (2009) 7051
20. A.P.I. Popoola, O.S.I. Fayomi, O.M. Popoola, *Int. J. Electrochem. Sci., 7* (2012) 4898
21. A.P.I. Popoola, O.S. Fayomi, *Sci. Rese. Essay.*, 6 (2011) 4264
22. B. Subramanian, S. Mohan, S. Jayakrishnan, *Surf. Coat. Technol., 201* (2006) 1145
23. O.S.I Fayomi, A.P.I Popoola, *Rese. Chem. Int.* ISSN 0922-6168 Res., (2013) Vol 39, N06 DOI 10.1007/s11164-013-1354-2
24. T. Frade, Z. Bouzon, A. Gomes, M.I. Da Silva, M.I Pereira, *Surf. Coat. Technol.*, 204 (2010) 3592